Laser-induced chemical vapor deposition of hydrogenated amorphous silicon. I. Gas-phase process model

M. Meunier,[a], J. H. Flint, J. S. Haggerty, and D. Adler[b]
Massachusetts Institute of Technology, Cambridge, Massachusetts 02139

(Received 17 March 1987; accepted for publication 9 June 1987)

In the laser-induced chemical vapor deposition (LICVD) process, a CO_2 laser beam impinges on a gas mixture parallel to the substrate upon which the film is deposited. Since heating of the reactant gases is accomplished only via the absorption of infrared photons, the reaction zone can be controlled precisely. The LICVD technique is a cold-wall thermal process allowing independent control of both the gas and substrate temperatures. In this paper, we propose a model for LICVD of silane (SiH_4) and growth of hydrogenated amorphous silicon (*a*-Si:H) thin films in which the film growth is controlled by gas-phase homogeneous thermal decomposition of the SiH_4. The peak gas temperature T_g depends on many process parameters, namely, gas partial pressures, laser power, substrate temperature, and cell geometry. Due to the extreme sensitivity of the growth rate G to the values of the partial pressures and laser power, these parameters must be fixed to within $\pm 1\%$ variation in order to control G to $\pm 50\%$ and prevent powder formation. LICVD gas-phase chemistry involves the production of SiH_2 for the thermal decomposition of SiH_4 and higher polysilanes (Si_2H_6, Si_3H_8, etc.) resulting from reactions between SiH_2 and SiH_4. SiH_2 and possibly higher diradicals produced in the laser beam then diffuse to the substrate and react with the surface layer, thus inducing growth of the *a*-Si:H film and the concomitant elimination of H_2.

I. INTRODUCTION

Several preparation techniques have been used to deposit hydrogenated amorphous silicon (*a*-Si:H) thin films. The most popular method is glow-discharge decomposition,[1] in which silane (SiH_4) is broken up by electric-field-induced collisions, creating a wide array of ions and neutral species which tend to produce significant concentrations of unannealed defects in the resulting films due to surface bombardment by the ions.[2,3] Another commonly used technique, reactive sputtering,[4] has a more intensive version of the same problem. In addition, interaction between the chamber walls and the plasma may lead to incorporation of unwanted impurities into the growing film in either of these methods. Thus, we might expect that a thermal process could be capable of producing higher-quality *a*-Si:H films, since the growth environment does not involve significant concentrations of high-energy particles.

Chemical vapor deposition (CVD) of SiH_4 has been used to prepare *a*-Si:H films,[5] but these films contain insufficient concentrations of H($[H] < 1$ at.%) to achieve good electronic properties because of the necessarily high substrate temperature ($T_s > 550$ °C). Due to their higher dissociation rates, higher silanes (Si_2H_6, etc.) have also been used to grow *a*-Si:H films by CVD processes but the starting gases are expensive and the resulting films do not appear to be of device quality at present.[6] In the laser-induced CVD (LICVD) process,[7–10] high deposition rates can be achieved at low substrate temperatures since the gas is heated by infrared photons in a region located a significant distance from the substrate. This produces films that contain adequate hydrogen and low defect concentrations.[8]

Figure 1 shows a schematic drawing of the LICVD technique. A CO_2 laser beam [$P(20)$ line, 10.591 μm] impinges on a gas mixture parallel to the substrate upon which the film is deposited. These reactant gases, which include SiH_4, are heated by absorbing infrared (IR) protons, so that the reaction zone can be controlled precisely. This allows the reactant gas temperature and the substrate temperature to be controlled independently. In addition, the cold-wall reactor eliminates contamination from the walls, a major problem of hot-wall reactors. The LICVD technique has similarities to the HOMOCVD process,[3,11–13] in which a cold substrate is placed in a hot-wall reactor, since both methods allow for independent control of the reactant gas and substrate tempertures and both proceed by the homogenous thermal dissociation of SiH_4. However, LICVD is subject neither to parasitic reactions near the hot walls nor to contamination from heated surfaces due to the high degree of spatial control possible with laser heating.

The use of lasers for semiconductor processing has become extremely popular over the last few years.[14] Photon frequencies ranging from IR to ultraviolet (UV) have been used to induce either pyrolytic or photolytic decomposition of molecules. In most of these processes, however, the laser beam is directed *perpendicular* to the substrate leading to

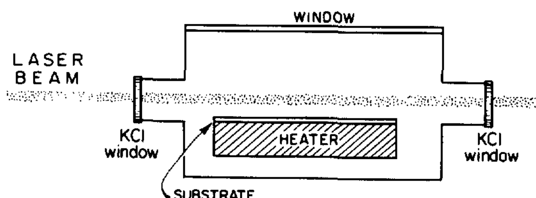

FIG. 1. Schematic of the LICVD reactor.

[a] Present address: Department of Engineering Physics, and Groupe des Couches Minces, Ecole Polytechnique de Montreal, Montreal, Quebec, Canada H3C 3A7.

[b] Professor David Adler died suddenly on March 31, 1987. We will long remember his precise thinking and vast culture, and most importantly his friendship for his collaborators.

 © 1987 American Institute of Physics

Downloaded 10 May 2002 to 132.207.124.22. Redistribution subject to AIP license or copyright, see http://ojps.aip.org/japo/japcr.jsp

thin-film growth via various local surface chemistries. Using this arrangement, Hanabusa *et al.*[15,16] deposited *a*-Si:H thin films with a CO_2 laser. In the perpendicular geometry, the laser beam heats both the SiH_4 gas and the substrate, creating small area films (~ 1 beam diameter, 6 mm) surrounded by powder. Since the CO_2 laser beam is *parallel* to the substrate in our geometry, the LICVD process produces films of much larger area, with the substrate temperature essentially decoupled from the gas temperature. Bilenchi *et al.*[17–20] have recently reported the deposition of *a*-Si:H by a technique similar to the one described here.

We have characterized our LICVD *a*-Si:H films, and have indeed found that their properties are primarily controlled by the substrate temperatures, as anticipated. These results are the subject of the companion paper.[21] In this paper, we describe the LICVD technique in detail and discuss the effects of varying the laser power, the SiH_4 partial pressure, and the carrier gas (Ar) pressure on both the gas absorptivity and the thin-film growth rate. The results are presented in Sec. II and are analyzed in Sec. III, in which a model for the process is presented. We find that the peak gas temperature T_g is primarily controlled by the SiH_4 partial pressure and the laser power. Our results suggest that the rate-limiting step in *a*-Si:H film growth is the gas-phase homogeneous thermal dissociation of SiH_4. The succeeding, more rapid steps are diffusion of the resultant SiH_2 and probably higher diradicals (e.g., Si_2H_4) to the substrate, surface reaction, elimination of hydrogen, and structural relaxation.

II. CHARACTERIZATION OF THE PROCESS

A. The deposition system

The deposition system is shown schematically in Fig. 1. Two different reactor cells have been used, one of which was described previously.[7] A modified apparatus has also been constructed in which the cell is in stainless steel and contains four IR-transparent KCl windows, which allow single-pass, collinear reflection of the transmitted beam as well as orthogonal crossing of two laser beams above the substrates. An Advanced Kinetics MIRL50 grading-tuned CO_2 laser is used in a cw mode on the $P(20)$ line (10.591 μm) with an available power of about 45 W. The axis of the unfocused beam is made to pass through the cell, parallel to the substrate plane at a distance of approximately one beam diameter (6 mm). A mirror can be placed at the exit window to reflect the laser beam back into the cell, thereby essentially doubling the power. Substrates are mounted horizontally on a temperature-controlled nickel-base block; we have investigated films with substrate temperatures in the 100–400 °C range.

The deposition system has electronic mass flowrate controllers for each of the gases used. Films have been deposited using either pure silane (at pressures in the range 4–9 Torr) with a flowrate of 2 standard cubic centimeters per minute (sccm) or a SiH_4/Ar mixture ($[Ar]/[SiH_4] = 1$) with a total flowrate of 4 sccm. The laser is turned on after the total pressure reaches 1–2 Torr. The pressure in the cell is then increased by closing the throttle valve between the reactor cell and the mechanical pump. Because of the strong dependence of gas absorptivity and growth rate on SiH_4 pressure, as is discussed in the next two subsections, film growth is ordinarily restricted to SiH_4 partial pressures P_{SiH_4} in the 4–9 Torr range.

B. Silane absorptivity

The SiH_4 absorptivity α is a function of the positions of its absorption lines, the laser emission lines, and their respective linewidths.[22] The CO_2 laser line that is maximally absorbed by SiH_4 is the $P(20)$ line (10.591 μm, $\nu_e = 944.195$ cm^{-1}),[23] which is near the SiH_4 absorption peak centered at $\nu_a = 944.213$ cm^{-1}.[24] Natural and Doppler broadening of the absorption line is insufficient to induce any coupling, so that the silane absorption is due to Lorentz or pressure broadening.[22]

The average gas absorptivity α over the beam path length l is defined as

$$W_{in} = W_{trans} \exp(-\alpha l), \quad (1)$$

where W_{in} and W_{trans} are the input and transmitted laser power, respectively. Figure 2 shows α as a function of P_{SiH_4} for two different nominal laser powers (8.8 and 36 W) and for two different Ar concentrations ($[Ar]/[SiH_4] = 0$, 1.2), as measured in the processing cell ($l = 17$ cm) with an unheated substrate. The increase of α with P_{SiH_4} is due to a pressure broadening effect. We find that $\alpha \propto (P_{SiH_4})^m$ with $m = 2$ when $P_{SiH_4} < 2$ Torr and $1.35 < m < 1.6$ when $P_{SiH_4} = 8$ Torr, a result that is discussed in greater detail in Sec. III. Although Ar is transparent to the laser beam, it has the effect of increasing α significantly by increasing the pressure broadening. The decrease of α with increase of laser power is most likely due to the effect of the increasing gas temperature on the absorption line.

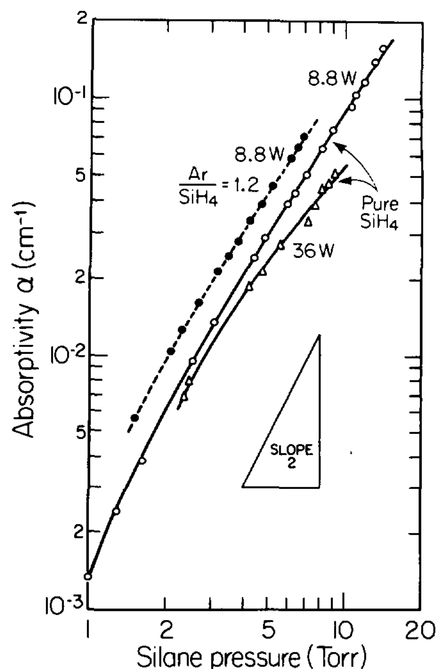

FIG. 2. SiH_4 absorptivity α(cm^{-1}) for the $P(20)$ CO_2 laser line as a function of SiH_4 partial pressure for nominal laser power 8.8 and 36 W and for $[Ar]/[SiH_4] = 0$ and 1.2.

Downloaded 10 May 2002 to 132.207.124.22. Redistribution subject to AIP license or copyright, see http://ojps.aip.org/japo/japcr.jsp

C. Growth rate

The growth is given by

$$G = \frac{\Delta d}{\Delta t} \text{ (Å/min)}, \tag{2}$$

where Δt is the elapsed time between successive appearances of red fringes at a particular point and Δd is the distance between these two fringes. Since $\lambda = 6500 \pm 250$ Å for red light and the *a*-Si:H index of refraction is $n = 4.3 \pm 0.3$,[25] $\Delta d = \lambda / 2n = 750 \pm 70$ Å.

Figure 3 shows the growth rate per Torr of SiH_4 [G/P_{SiH_4} (Å/min/Torr)] as a function of P_{SiH_4} for various laser powers W_z at two substrate temperatures, $T_s = 300$ and 350 °C, for both pure SiH_4 and for an Ar/SiH_4 mixture with $X \equiv [Ar]/[SiH_4] = 1.0$. The observed growth rates, $G = 10$–300 Å/min, are of the same order of magnitude as those obtained using glow-discharge techniques.[1] G increases by an order of magnitude when either W_z increases by $\approx 25\%$ or P_{SiH_4} increases by $\simeq 10\%$. Admixing Ar has the effect of decreasing the P_{SiH_4} and increasing the maximum growth rate by a factor of 5 for a change from $X = 0$ to $X = 1$. In contrast, an increase in T_s from 300 to 350 °C increases the growth rate by less than a factor of 2.

It is clear from these results that the main parameters controlling the growth mechanism in LICVD are P_{SiH_4}, the Ar partial pressure P_{Ar}, and W_z; T_s has only a small effect on G. These results can all be understood by considering the effects of these parameters on the gas temperature, which controls the SiH_4 decomposition rate. The gas temperature increases whenever additional photons are absorbed by the gas, and this can be accomplished by increasing either the laser power or the gas absorptivity. Moreover, the gas absorptivity is a strong function of both P_{SiH_4} and P_{Ar}, as is evident from Fig. 2. The results of Figs. 2 and 3 form the basis of the process model proposed in Sec. III.

In any event, the growth-rate results shown in Fig. 3 have important implications for the LICVD process. Due to the extreme sensitivity of G on P_{SiH_4} and W_z these parameters must be controlled to within a 1% maximum variation. The laser power is usually stable to within $\pm 1\%$, but electronic mass-flow controllers are essential in order to prevent significant variations in P_{SiH_4} and P_{Ar}. In fact, the previously reported[7] spread in growth rates with time is very likely due to uncontrolled variations of P_{SiH_4}.

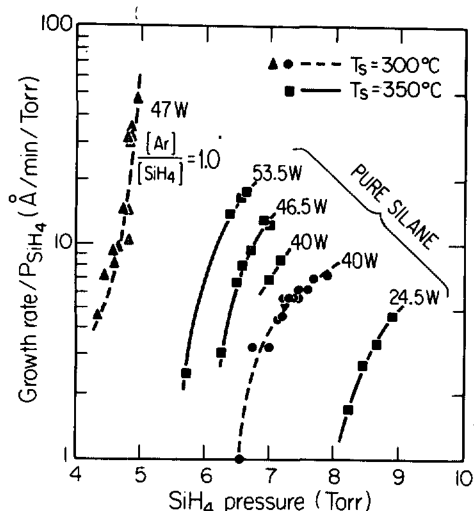

FIG. 3. Growth rate (Å/min) per Torr of SiH_4 as a function of P_{SiH_4} (Torr) in various processing conditions. Powers are calculated for positions above the substrate.

D. Film thickness uniformity

The *a*-Si:H films produced by LICVD are not uniform over a 25×50 mm^2 substrate, but typically have maximum thickness of 0.5–2.0 μm. If we take the x and y axes as the directions parallel and perpendicular to the laser beam, respectively, we find that there is a slight spread in film thicknesses in the x direction, probably due to a variation of T_g along the laser beam arising from variations in W_z. This leads to a maximum thickness variation of $\pm 25\%$ for a substrate 50 mm long. However, the spread in thickness in the y direction is usually more pronounced. Figure 4 shows a typical thickness profile as a function of y for a film deposited at $T_s = 300$ °C in pure SiH_4. For this particular film, the laser beam was reflected back into the cell at a slight angle from the incident beam, such that the reflected beam was 2 mm from the incident beam and both beams were 6 mm from the substrate. The film thickness decreased by a factor of 2.5 over a 10-mm width. More uniform films can be obtained by scanning the laser beam[20] or by rolling a flexible substrate onto the heated block.

III. A MODEL FOR LICVD OF *a*-Si:H FILMS

Due to basic similarities with the HOMOCVD process,[11,12] it is reasonable to infer that the LICVD process proceeds essentially thermally, with G controlled by the pyrolysis of SiH_4. The resulting SiH_2 diradicals and possibly higher diradicals then diffuse from the laser beam to the substrate where the film is formed. Thus, G should be exponentially dependent on T_g, while the film properties should depend primarily on T_s, which can be independently controlled. We also anticipated that T_g is determined by the various process parameters, primarily W_z, P_{SiH_4}, and P_{Ar}.

A complete model for the process requires: (i) analysis of the interactions between the IR photons and the SiH_4 molecules; (ii) calculation of the gas temperature from the

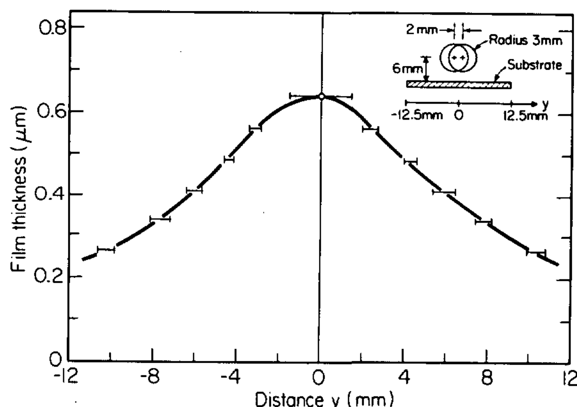

FIG. 4. Film thickness variation as a function of the distance y for a film processed at $T_s = 300$ °C in pure SiH_4. The laser beam has been reflected back into the cell as shown in the insert of the figure.

Downloaded 10 May 2002 to 132.207.124.22. Redistribution subject to AIP license or copyright, see http://ojps.aip.org/japo/japcr.jsp

steady-state energy balance; (iii) analysis of the reaction kinetics, which can be obtained from Arrhenius plots of G as a function of T_g; and (iv) understanding the dependence of the LICVD process on the various process parameters. These are discussed in detail in the following four subsections.

A. Photon-molecule interactions

When an infrared photon is absorbed, the SiH_4 molecule makes a transition to an excited vibrational level. Collisions distribute the absorbed energy and return the absorbing molecule to the ground state, where it is again able to absorb another photon.[26] For the conditions used in LICVD (input intensity 160 W/cm^2; absorbed power ~ 1 W/cm at $P_{SiH_4} \sim 10$ Torr and with $T_g \approx 800$ K), a molecule absorbs a photon every 700 μs. The average time between intermolecular collisions τ_{coll} is ~ 0.015 μs; thus a molecule makes $\sim 45\,000$ collisions before absorbing another photon. It has been estimated[26,27] that at $P_{SiH_4} \sim 10$ Torr, the vibrational-vibrational, vibrational-rotational, and vibrational-translational relaxation times are 0.5, 100, and 100 μs, respectively. Therefore, the molecules will have adequate time to relax through collisions to a state where the absorbed vibrational energy is distributed almost equally among the various degrees of freedom of the molecule. Thus, the gas returns to a state of thermal equilibrium between successive absorptions, and the overall result of photon absorption is an increase in T_g.

Hanabusa and Kikuchi[28] have done a coherent anti-Stokes Raman (CARS) study of LICVD. The CARS spectrum of SiH_4 is unique in that it contains an additional peak, which was interpreted as arising from rotationally excited molecules following gas reactions. A similar peak was noted when the gas is heated normally. Thus, the special feature is related not to the way the gas is heated but rather to how the SiH_4 dissociates, and it is impossible to estimate T_g from CARS. This result is not in contradiction with our conclusion that LICVD is a thermal process.

Deutsch[23] and Longeway and Lampe[27] have studied the IR photochemistry of silane extensively. Using a pulsed CO_2 laser ($\sim 10^7$ W/cm^2) with a pulse time 100–200 ns, both groups reported that the average number of photons absorbed per molecule during a pulse varies between 1.5 ($P_{SiH_4} = 1$ Torr) and 7.5 ($P_{SiH_4} = 10$ Torr). Longeway and Lampe[27] tentatively concluded that SiH_4 decomposition can occur from multiple photon absorption up to the quasi-continuum. With the high laser intensity used, the time between two successive absorptions by a molecule is of the same order of magnitude as the collision time. Therefore, the molecules have insufficient time to relax. However, with the much lower laser intensity used in the LICVD process (10^2 W/cm^2), the gas molecules experience sufficient collisions to justify the thermal equilibrium description.

Because of the difference between the emission line ($\nu_e = 944.195$ cm^{-1}) and the absorption line ($\nu_a = 944.213$ cm^{-1}), collisions are necessary to broaden the SiH_4 rotational level sufficiently to have appreciable absorption.[22] The cross section σ_c of the molecule will be a function of the frequency mismatch and the Lorentz or pressure broadening, $\Delta\nu_L \propto (1 + \beta X) P_{SiH_4}$, where βX is the additional contribution to the broadening by another gas (for Ar, $X = [Ar]/[SiH_4]$ and $\beta = 0.8278$).[22,29] With $P_{SiH_4} \sim 10$ Torr, the pressure broadening ($\Delta\nu_L \approx 0.003$ cm^{-1}) is smaller than $|\nu_e - \nu_a| = 0.018$ cm^{-1}. Therefore, the Lorentz line shape can be written[22]

$$\sigma_c \propto \frac{\Delta\nu_L}{(\Delta\nu_L)^2 + (\nu_e - \nu_a)^2} \simeq \frac{\Delta\nu_L}{(\nu_e - \nu_a)^2}. \quad (3)$$

Since the absorptivity is $\alpha = N\sigma_c$, where N is the number of absorbing molecules $[N = P_{SiH_4}(kT_g)^{-1}]$,

$$\alpha(\mathbf{r}) = (1 + \beta X) P_{SiH_4}^2 F[T(\mathbf{r})], \quad (4)$$

where $F(T)$ is a function of the gas temperature only and depends on level populations and gas density variations with temperature. It is clear from Eq. (4) that the fact that the gas temperature varies with position induces a spatial distribution in $\alpha(\mathbf{r})$. However, the measured absorptivity is an average of $\alpha(\mathbf{r})$ over the entire path length.

From Fig. 2, it is clear that the averaged absorptivity is given by $\alpha \sim (P_{SiH_4})^m$, where $m \approx 2$ at low pressures ($P_{SiH_4} < 2$ Torr), but decreases to about 1.5 at higher pressure (> 8 Torr). The variation of m with P_{SiH_4} is due to the variation of $F(T)$ with P_{SiH_4}. Indeed, at low pressures, the gas absorptivity is low and the gas remains relatively cool. Consequently, in this range, the gas temperature is only a slowly varying function of α. Then $F(T)$ is relatively constant, and Eq. (4) shows that $m = 2$. However, at higher pressures, α is much larger, the gas heats up considerably, and the distribution $F(T)$ changes the value of m. Since $m < 2$, $F(T)$ has the effect of decreasing the absorptivity when the gas temperature increases.

B. The gas temperature

T_g is calculated from an analysis of the steady-state energy balance, where the energy absorbed by the gas is set equal to the energy lost due to thermal conduction.[10] With our parameters (flowrate $\approx$ 2–4 sccm and $P_{SiH_4} \sim 10$ Torr), the energy lost by forced convection is about a factor of 10^3 smaller than by thermal conduction. The heat of the reaction can be neglected, since only a small fraction ($< 1\%$) of the gas is dissociated. Moreover, the energy lost by thermal radiation is negligible due to the long IR emission lifetime ($\sim$ 1–100 ms $\gg \tau_{coll}$). We have also verified that the mean free path (≈ 0.001 cm) is much smaller than any dimension in the cell, including the laser-beam-to-substrate distance (0.6 cm). Therefore, the steady-state energy balance is[30]

$$\nabla \cdot \{-\kappa[T(\mathbf{r})] \nabla T(\mathbf{r})\} = \alpha(\mathbf{r}) I(\mathbf{r}) \quad (\mathrm{W/cm^3}), \quad (5)$$

where $T(\mathbf{r})$ is the gas temperature as a function of position $\mathbf{r}$ and $\alpha(\mathbf{r})$ is the absorptivity in cm^{-1}. Values for the gas thermal conductivity $\kappa(T)$ can be fit to a relation of the form[29]

$$\kappa(T) = \kappa_0 (T/T_R)^n \quad (\mathrm{W/cm\,K}), \quad (6)$$

where T_R is a reference temperature around which Eq. (6) is valid. For pure SiH_4, $\kappa_0 = 8.6 \times 10^{-4}$ W/cm K and $n = 1.25$ for $T_R = 800$ K.[29] If the beam has a gaussian shape, the intensity I(W/cm^2) is given by

Downloaded 10 May 2002 to 132.207.124.22. Redistribution subject to AIP license or copyright, see http://ojps.aip.org/japo/japcr.jsp

$$I(x,y,z) = W_z(\pi R^2)^{-1} \times \exp\{-[(x-x_0)^2 + (y-y_0)^2]/R^2\}, \quad (7)$$

where R is the beam radius, the z axis is in the beam direction, W_z is the power at z, and x_0 and y_0 give the position of the beam center.

Figure 5 shows the results of a two-dimensional computer calculation of the gas temperature variation in the direction perpendicular to the substrate and passing through the beam center for various absorbed powers (W/cm) and substrate temperatures. Increasing the absorbed power from 0 to 1 W/cm by either increasing the P_{SiH_4} or the input power increases the peak gas temperature T_g at the beam center ($x = 30$ mm) from ~ 200 to 610 °C when $T_s = 300$ °C. However, with $\alpha W = 1$ W/cm, increasing T_s from 200 to 400 °C increases T_g at the beam center from 580 to 660 °C. Film growth at low values of T_s requires an increase in absorbed power in order to compensate for the energy lost to the substrate. In the Appendix, we show that T_g follows the relation [see Eq. (A7)]:

$$\left(\frac{T_g}{aT_R}\right)^{n+1} - \left(\frac{T_s}{bT_R}\right)^{n+1} - \left(\frac{T_w}{cT_R}\right)^{n+1} = \frac{(n+1)\alpha W_z}{\pi\kappa_0 T_r}, \quad (8)$$

where T_w and T_R are the wall and reference temperatures, respectively ($T_w = 300$ K, $T_R = 800$ K), a, b, and c are geometrical factors, and n is defined in Eq. (6).

Equation (8) shows that αW_z above the substrate is necessary for the calculation of the gas temperature at any specific point. However, as pointed out previously the measured α is actually the averaged value over the beam path length (≈ 17 cm), so that this value yields an incorrect estimate for T_g above the substrate. Nevertheless, we expect that the W_z calculated from an averaged α should give a good estimate of the power at the point of interest. Parameters like P_{SiH_4} and P_{Ar} should be used, since they are position independent. These pressures, along with the calculated W_z, are used to calculate T_g above the substrate by the method described below.

By combining Eqs. (4) and (8), we obtain

$$\left(\frac{T_g}{aT_R}\right)^{n+1} - \left(\frac{T_s}{bT_R}\right)^{n+1} - \left(\frac{T_w}{cT_w}\right)^{n+1} = \frac{(n+1)}{\pi T_R} \frac{(1+\beta X) W_z P_{SiH_4}^2}{\kappa_0} F(T_g). \quad (9)$$

Equation (9) shows that T_g is only a function of $(1+\beta X) W_z (P_{SiH_4})^2 \kappa_0^{-1}$ and T_s for a specific system geometry (a, b, c, T_w and T_R are constants). Figure 6 shows G/P_{SiH_4} as a function of $(1+\beta X) W_z P_{SiH_4}^2 (\kappa_{mix}/\kappa_{SiH_4})^{-1}$ for the data of Fig. 3. Continuous curves are obtained for $T_s = 350$ °C (pure SiH_4 with several different values of W_z) and $T_s = 300$ °C (pure SiH_4 and an Ar/SiH_4 mixture), in agreement with the model. The function $F(T_g)$ in Eq. (9) is needed to calculate T_g from the various measurable parameters. Assuming that the only effect of the substrate temperature is to change T_g and that the growth rate is a unique function of T_g, we can calculate $F(T_g)$ from the data of Fig. 6, which gives various values of T_s and $(1+\beta X) W_z P_{SiH_4}^2 (\kappa_{mix}/\kappa_{SiH_4})^{-1}$ for a specific peak gas temperature. Using Eq. (9), we find that $F(T_g)$ obeys the empirical relation:

$$F(T_g) = 2.7\times 10^{-4} (T_g/T_R)^{-0.46} \quad (\text{cm}^{-1}/\text{Torr}^2) \quad (10)$$

for $730 < T_g < 840$ K.

With this expression for $F(T_g)$, the gas absorptivity above the substrate takes the form

$$\alpha = 2.7\times 10^{-4} (1+\beta X) P_{SiH_4}^2 (T_g/T_R)^{-0.46} \quad (\text{cm}^{-1}), \quad (11)$$

where P_{SiH_4} is in Torr, $T_R = 800$ K, and $\beta = 0.8278$ for Ar. As P_{SiH_4} or W_z increases, T_g increases, which by Eq. (11) reduces α. This is in agreement with our observations that $\alpha \propto (P_{SiH_4})^m$ with $m = 2$ for $P_{SiH_4} < 2$ Torr and $m \approx 1.6$–1.35 for $P_{SiH_4} = 8$ Torr (see Fig. 2). However, due to the fact that we measure an average α for a beam path over which T_g might vary significantly, we cannot expect perfect agreement between the measured and the calculated values of α.

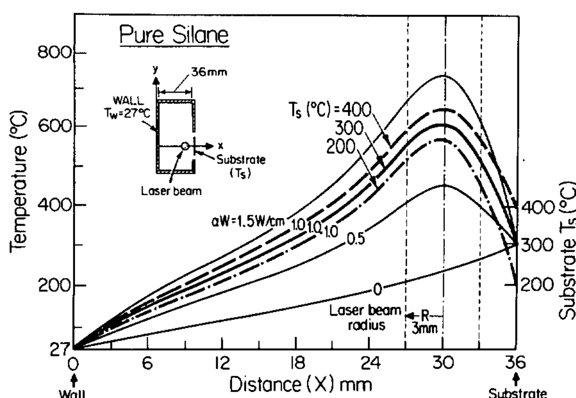

FIG. 5. Two-dimensional computer calculation of the gas temperature variation in the direction perpendicular to the substrate and passing through the beam center for absorbed powers $\alpha W = 0$, 0.5, 1.0, 1.5 W/cm and for substrate temperatures $T_s = 200$, 300, 400 °C ($\alpha W = 1.0$ W/cm).

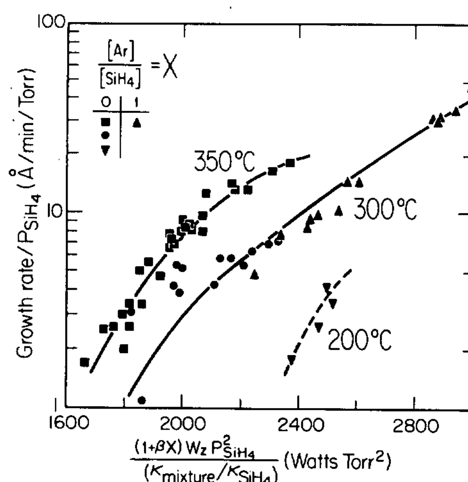

FIG. 6. Growth rate (Å/min) per Torr of SiH_4 as a function of $(1+\beta X) W_z P_{SiH_4}^2 (\kappa_{mix}/\kappa_{SiH_4})^{-1}$ (W Torr²) for $T_s = 200$, 300, and 350 °C.

Downloaded 10 May 2002 to 132.207.124.22. Redistribution subject to AIP license or copyright, see http://ojps.aip.org/japo/japcr.jsp

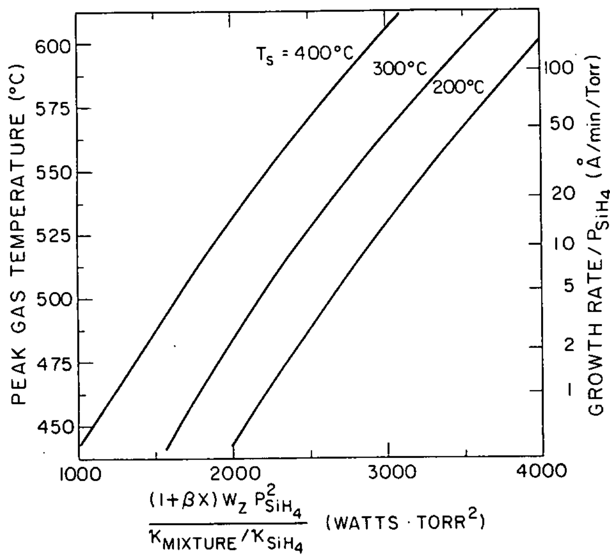

FIG. 7. Calculated peak gas temperature as a function of $(1+\beta X)\, W_z P^2_{\text{SiH}_4} (\kappa_{\text{mix}}/\kappa_{\text{SiH}_4})^{-1}$ for various substrate temperature for $a = 0.9566$, $b = 1.1152$, $c = 1.9328$, and $n = 1.25$. Growth rate values are from Fig. 8.

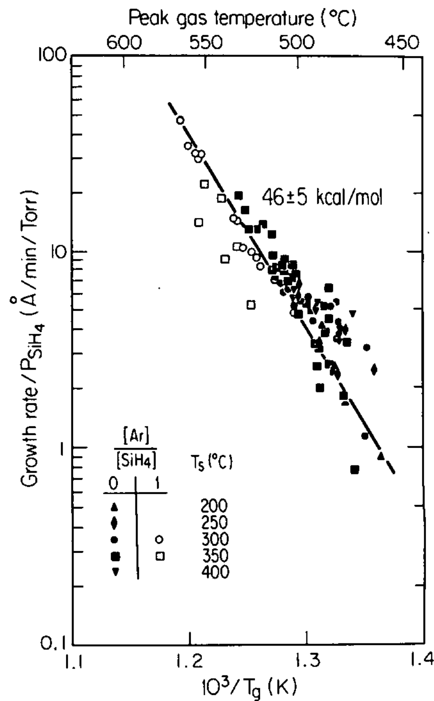

FIG. 8. Arrhenius plot of growth rate (Å/min) per Torr of SiH_4 as a function of reciprocal calculated peak gas temperature for films made in various processing conditions.

In any event, Eq. (11) gives the gas absorptivity above the substrate for $730 < T_g < 840$ K.

Combining Eqs. (9) and (10), we obtain

$$\left(\frac{T_g}{aT_R}\right)^{n+1} - \left(\frac{T_s}{bT_g}\right)^{n+1} - \left(\frac{T_w}{cT_R}\right)^{n+1} = 2.7\times 10^{-4}\frac{(n+1)}{\pi T_R}\frac{(1+\beta X)W_z P^2_{\text{SiH}_4}}{\kappa_0}\left(\frac{T_g}{T_R}\right)^{-0.46} \quad (12)$$

This relation is general and gives T_g as a function of measurable quantities, $P_{\text{SiH}_4}, W_z, X, T_s$, and geometry (i.e., $a,b,c,$). For our specific system geometry, shown in the insert of Fig. 5 ($a = 0.9566$, $b = 1.1152$, and $c = 1.9328$), the calculated values of T_g as a function of $(1+\beta X)\, W_z P^2_{\text{SiH}_4} (K_{\text{mix}}/K_{\text{SiH}_4})^{-1}$ for several values of T_s are plotted in Fig. 7. These results can then be used to calculate T_g as a function of $T_s, W_z, P_{\text{SiH}_4}$, and X.

C. Reaction kinetics

Figure 8 shows the Arrhenius plot of G/P_{SiH_4} as a function of the reciprocal of T_g for 80 different runs made under various processing conditions ($4 < P_{\text{SiH}_4} < 10$ Torr, $200\,°\text{C} < T_s < 400\,°\text{C}$, $25\ \text{W} < W_z < 54$ W, and $X = 0,1$). There is some scatter in the data which should be expected because of small variations in both the geometry (e.g., laser-beam-to-substrate distance) and the laser mode during different runs. However, for all the runs, G can be expressed approximately as

$$\log\left(\frac{G}{P_{\text{SiH}_4}}\right) = 13.6 \pm 1.3 - \left(\frac{(46 \pm 5\ \text{kcal/mol})}{2.3RT_g}\right)\left(\frac{\text{Å/min}}{\text{Torr}}\right) \quad (13)$$

in the gas temperature range 450–575 °C.

The observed activation energy of 46 ± 5 kcal/mol is close to both the single-pulse shock tube kinetics results of 52.7 kcal/mol for the silane decomposition[31] (pressure $\simeq 4000$ Torr and $T = 762$–911 °C) and to the static experiment results of 56 kcal/mol for the same reaction[32] (pressure = 35–230 Torr and $T = 375$–430 °C). The LICVD result is also close to the 53.9 kcal/mol for G in the HOMOCVD process[11,12] where is has been proposed that SiH_2 resulting from the thermal decomposition of SiH_4 is the main precursor of film deposition. From kinetics studies,[31,32] the initial reaction for the SiH_4 pyrolysis is

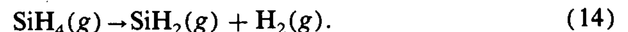

$$\text{SiH}_4(g) \rightarrow \text{SiH}_2(g) + \text{H}_2(g). \quad (14)$$

Small differences exist between LICVD activation energies and the one required for the pyrolysis of SiH_4 and is probably due to differences in experimental conditions. Indeed, the rate constant for reaction (14) is in the pressure fall-off region and kinetics parameters should therefore depend on pressure, type of gas and also on temperature. Recently, Coltrin, Lee, and Miller[33] did an empirical fit to the temperature and pressure dependence of the silane unimolecular decomposition rate constant obtained from RRKM analysis of the experimental data of Newman *et al.*[31] The results are on the form

$$k = (a + bP)AT^{\beta}\exp(-E/RT), \quad (15)$$

where $a = 0.0504$, $b = 0.9496$, $\beta = -7.95$, $E = 61.96$ kcal/mol, $A = 2.54\times 10^{38}\ \text{s}^{-1}$, and P is the total pressure in atmosphere (5 Torr $< P <$ 1 atm). With our particular conditions for the LICVD process (5 Torr $< P <$ 10 Torr and $450\,°\text{C} < T < 575\,°\text{C}$) Eq. (15) can be approximated by

$$k = 1.57\times 10^{14}\exp(-49.6 \pm 0.8\ \text{kcal/mol}/RT)\ (\text{s}^{-1}). \quad (16)$$

In the LICVD conditions, the activation energy for the formation of SiH_2 is within experimental error of the observed

Downloaded 10 May 2002 to 132.207.124.22. Redistribution subject to AIP license or copyright, see http://ojps.aip.org/japo/japcr.jsp

LICVD activation energy of 46 ± 5 kcal/mol. Finally, note that the involvement of SiH_3 in SiH_4 pyrolysis is excluded since its formation energy is approximately 40 kcal/mol larger than that for the formation of SiH_2.

According to Scott, Reimer, and Longeway,[34] other gas-phase reactions should follow reaction (14), including the formation of higher silanes Si_2H_6, Si_3H_8,...resulting for instance from the reactions between SiH_2 and SiH_4, Si_2H_6, or higher silanes. These reactions have very low activation energies of the order of 2 kcal/mol.[35] However, these higher silanes should decompose back to form SiH_2 and higher diradicals (e.g., SiH_3SiH,...). For instance, thermal decomposition of Si_2H_6 produces SiH_2 with $E = 49.8$ kcal/mol (Ref. 36) and decomposition of Si_3H_8 leads to SiH_2 with $E = 53$ kcal/mol or SiH_3SiH with $E = 49$ kcal/mol.[37] Again these activation energies are of the same order of magnitude of the one for the LICVD growth process.

Modeling the LICVD process is difficult since many intermediate reaction-rate constants in the pyrolysis of SiH_4 are unknown. However, the relatively good agreement between the observed activation for the growth in the LICVD process and the one for thermal decomposition of silane and higher silanes suggests that the LICVD *a*-Si:H film growth results from the pyrolysis of SiH_4. Silene (SiH_2) and probably higher diradicals diffuse from the laser beam to the film surface leading to the film growth. However, as pointed out by Scott, Reimer, and Longeway,[34] those diradicals diffusing toward the cold substrate react with SiH_4 to form cold polysilanes as the gas temperature decreases from the hot zone (i.e., within the laser beam) to the cold substrate. All of these reactions complicate the development of a quantitative model of the gas-phase chemistry occurring in the LICVD process. However, some insight can be obtained by comparing the proposed model with some assumptions to the film thickness variation of Fig. 4.

Let C_i be the concentration of diradicals (SiH_2, SiH_3SiH,...). Then, equation of continuity for that particular species is

$$\frac{dC_i}{dt} = D_i \nabla^2 C_i - R_i, \tag{17}$$

where we assume a constant diffusion coefficient D_i for species i and R_i represents all possible reactions mentioned above that produce and consume that species. The magnitude of the corresponding growth rate G_i is its flux at the film surface times the appropriate number of Si atoms N_i divided by the *a*-Si:H film density ($\rho = 5 \times 10^{22}\ \mathrm{cm}^{-3}$):

$$G_i = (N_i D_i/\rho) \nabla C_i |_{\text{film surface}}. \tag{18}$$

The total growth rate is

$$G = \rho^{-1} \nabla Z, \tag{19}$$

where

$$Z = \sum_i N_i D_i C_i. \tag{20}$$

In steady state, Eq. (17) becomes for all species

$$\nabla^2 Z = \sum_i N_i R_i. \tag{21}$$

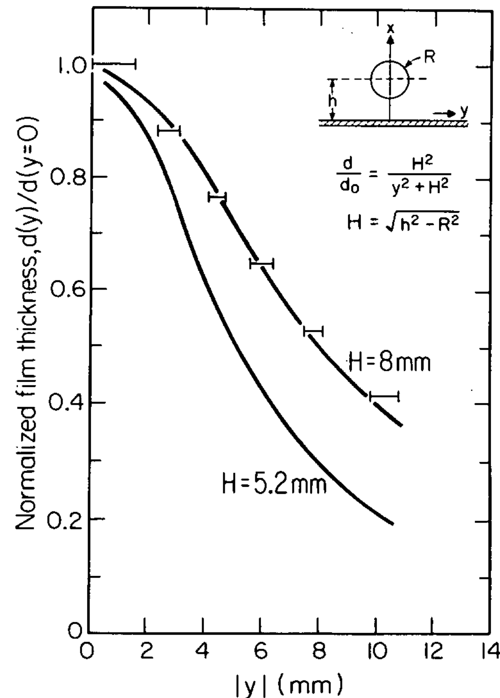

FIG. 9. Normalized film thickness $d(y)/d(y=0)$ as a function of y (mm).

Now, a particular diradical might be consumed to produce a higher silane which in turn might dissociate back to form the original diradicals or some other diradicals. Since we would expect the summation over all diradical species of the difference between the production and consumption terms to be negligible compared to the diffusion term, our calculation should lead to an estimate of the flux at the film surface. With this assumption, Eq. (21) becomes

$$\nabla^2 Z = 0. \tag{22}$$

This has to be solved for our particular geometry. Let h be the vertical distance from the film surface to the center of the laser beam of radius R, and let the y axis be perpendicular to the beam axis and parallel to the film surface and the x axis be perpendicular to the film surface and passing through the axis of the beam (see the inset of Fig. 9). If the surface concentration of diradicals is negligible (i.e., fast surface reactions), the calculated growth rate is[38]

$$G = \frac{2Z_{\text{beam}}}{\rho H \ln[(h+H)/R]} \left(\frac{H^2}{y^2 + H^2}\right), \tag{23}$$

where $H = (h^2 - R^2)^{1/2}$. Z_{beam} is Eq. (20) evaluated in the beam and is a very difficult quantity to estimate without an exact knowledge of all possible reactions occurring in the gas. However, this quantity is not important if we consider only the film thickness variation $d(y)$ which according to Eq. (23) follows

$$\frac{d(y)}{d(0)} = \frac{H^2}{y^2 + H^2}. \tag{24}$$

Films grown by the LICVD process are not uniform in thickness, as is clear from Fig. 4. Figure 9 shows the normalized film thickness, $d(y)/d(0)$, compared with the estimates from Eq. (24) with $H \equiv \sqrt{h^2 - R^2} = 5.2$ and 8 mm. The choices of $h = 6$ mm and $R = 3$ mm ($H = 5.2$ mm) result in

Downloaded 10 May 2002 to 132.207.124.22. Redistribution subject to AIP license or copyright, see http://ojps.aip.org/japo/japcr.jsp

a theoretical curve that is lower than the experimental data. This is most likely due to our assumption of only negligible overall gas-phase chemistry. It is probable that SiH_2 generated in the gas phase readily inserts into SiH_4 to form Si_2H_6, which is more reactive than SiH_4 and brings two Si atoms to the surface. Thus, since gas-phase chemistry has a net positive contribution to the growth rate, we might expect that our predicted curve is smaller than the observed one. In any event, if we choose $H = 8$ mm, good agreement between the calculation and the data is obtained. It is important to point out that our films were processed using a reflected beam having a 2 mm shift in the y direction (see the inset of Fig. 4). Equation (24) was derived using a beam of radius R located at $x = h$ from the film surface. The results of Fig. 9 suggest that the "effective" laser beam of our reflected-beam geometry has $H = 8$ mm. This can be represented by $h = 8$ mm ($R = 0$ mm) up to $h \approx 8.5$ mm ($R = 3$ mm). The effective location of the diradicals source is within the region in which the two beams overlap and about 2.0–2.5 mm above the centers of two beams.

LICVD and HOMOCVD are both thermal processes based on the formation of SiH_2 species. This is different from the process of plasma decomposition, in which there is experimental evidence that SiH_3 is the main precursor in the film deposition.[34,39,40] Scott, Reimer, and Longeway[34] have suggested that in HOMOCVD there is a possible source of SiH_3, from reactions on the surface of the hot walls of the reactor. However, LICVD is a cold-wall reactor technique, and the presence of monoradicals in the gas is highly improbable. The possible involvement of SiH_3 in HOMOCVD might explain the small differences between the observed properties of films produced by the HOMOCVD and LICVD processes.

D. Control of the LICVD process

In the LICVD process, the CO_2 laser is used to heat up and thermally decompose the silane. The gas temperature T_g is critical; in turn, T_g depends on the silane and argon partial pressures, P_{SiH_4} and P_{Ar}, and the laser power above the substrate W_z. Using Eq. (13) and assuming $T_g \approx 800$ K, we find that the variation of the growth rate with the gas temperature is

$$\Delta G/G = 30(\Delta T_g/T_g). \tag{25}$$

Thus, a change of about 3% in T_g leads to a variation in G of approximately a factor of 2. Using Eq. (12) with $n = 1.25$ and neglecting the T_s and T_w terms, we can calculate that T_g varies with the process parameters as

$$\frac{\Delta T_g}{T_g} \approx \frac{1}{2.71}\left(2\frac{\Delta P_{SiH_4}}{P_{SiH_4}} + \beta\frac{\Delta P_{Ar}}{P_{Ar}} + \frac{\Delta W_z}{W_z} - \frac{\Delta\kappa_0}{\kappa_0}\right). \tag{26}$$

The variation of G with these parameters is then

$$\frac{\Delta G}{G} \approx 22\frac{\Delta P_{SiH_4}}{P_{SiH_4}} + 9\frac{\Delta P_{Ar}}{P_{Ar}} + 11\frac{\Delta W_z}{W_z} - 11\frac{\Delta\kappa_0}{\kappa_0}. \tag{27}$$

If variations in the partial pressures and the laser power are of the order of 1% (as might be expected under the conditions used in our system), then G can fluctuate by $\approx 50\%$. This is consistent with both the observations of Bilenchi *et al.*[19] and our data shown in Fig. 3, for which G increases by about a factor of 2 as the power increases by 9%.

Some constant volume (static cell) experiments were carried out,[7] and indicated that as the film begins to be deposited, G decreases to zero rapidly. This is due to the fact that $H_2(g)$ is a product of reactions which increase the gas thermal conductivity, leading to a sharp decrease in T_g. For instance, an increase in the H_2 partial pressure from 0 to 1% increases κ_{gas} by 10%,[29] leading to a decrease of G by more than a factor of 2. A flowing gas system is necessary to remove the H_2 from the gas. We also previously reported a dependence of G on the flowrate.[7] This may be due either to a change in gas thermal conductivity or to an unmonitored pressure variation which results in an uncontrolled flowrate.

Similar to HOMOCVD and glow-discharge decomposition, the maximum growth rate in LICVD is controlled by the onset of powder formation. The role of gas-phase nucleation on the CVD process has been discussed previously by Sladek.[41] At high values of either P_{SiH_4} or T_g, gas-phase reactions involving high radical concentrations lead to the formation of aggregates. In the LICVD process, T_g is determined by P_{SiH_4} and W_z. Control of P_{SiH_4} and W_z to within $\pm 1\%$ is required to prevent any major variations in T_g which might produce powder instead of film.

The effect of Ar on the LICVD process is both to decrease the gas thermal conductivity and to broaden the SiH_4 absorption lines. These result in Ar/SiH_4 mixtures yielding the same values of T_g and G at lower P_{SiH_4} than in the case of pure SiH_4. As is evident from Fig. 3, the incorporationof Ar has the beneficial effect of increasing G by about a factor of 5 (for 47 W), by lowering P_{SiH_4} from 7 to 5 Torr as X increases from 0 to 1. From the same figure, we can also see that an increase in W_z from 24.5 to 53.5 W increases the maximum value of G from 45 to 120 Å/min by lowering P_{SiH_4} from 9 to 7 Torr. These results suggests that lower P_{SiH_4} moves the onset of powder formation to higher gas temperatures, leading to higher film growth rates.

IV. CONCLUSIONS

LICVD is a cold-wall thermal process in which G is controlled by the thermally activated dissociation of SiH_4 at a rate determined by T_g. The balance between the energy absorbed by the gas molecules and that lost to the surrounding surfaces by thermal conduction determines T_g. The specific value of T_g depends on gas characteristics and on many process parameters including P_{SiH_4}, W_z, X, T_s, and geometry. Due to the extreme sensitivity of the process to several of these parameters, P_{SiH_4} and W_z have to be controlled to within a $\pm 1\%$ variation in order to control the growth rate to $\approx \pm 50\%$ and prevent powder formation. The maximum growth rate is limited by the onset of powder formation, which in turn is related to T_g and P_{SiH_4}.

Similar to the HOMOCVD process, the gas-phase chemistry involves the production of SiH_2 from thermal decomposition of SiH_4 and higher polysilanes (Si_2H_6, Si_3H_8, etc.) which arise from reactions between SiH_2 and SiH_4. SiH_2 and possibly higher diradicals produced in the laser beam then diffuse to the substrate and insert into any of the

Downloaded 10 May 2002 to 132.207.124.22. Redistribution subject to AIP license or copyright, see http://ojps.aip.org/japo/japcr.jsp

Si–H bonds of the hydrogenated surface, leading to the growth of *a*-Si:H films and the elimination of hydrogen. In our model, all the succeeding steps are rapid compared to the thermal decomposition of SiH_4 in the laser beam.

Our results suggest that the use of higher laser power or a gas with lower thermal conductivity provides a good method for retarding the onset of powder formation, thus leading to higher film growth rates. More uniform films can be obtained by either scanning the laser parallel to the substrate or by rolling a flexible substrate under a fixed laser. We expect that the LICVD process might be applicable to the production of other materials for which a cold-wall thermal processes with independently controlled T_g and T_s is desirable; for example, Si_3N_4 and SiO_2 can be produced by incorporating appropriate gases (e.g., NH_3, O_2, ...) in specific concentrations. A careful analysis of the gas chemistry as well as the effects of the gases on the pressure broadening, gas thermal conductivity, and gas temperature is essential.

ACKNOWLEDGMENTS

We would like to thank Dr. T. R. Gattuso, who carried out much of the pioneering work on the LICVD process. We are also grateful to Dr. J. D. Casey and R. Fenner for their contribution to this work and to Professor H. K. Bowen and R. W. Field for many helpful discussions. This research was partially supported by the 3M Corporation and the Semiconductor Research Corporation. One of us (M. M.) would like to acknowledge the generous financial aid he received from the National Research Council of Canada, the Quebec Ministry of Education, and the Standard Oil Co. (SOHIO).

APPENDIX

The differential equation, Eq. (5), which describes the steady-state energy balances in the LICVD process can be linearized by the Kirchhoff transformation[30]:

$$\theta = \frac{(n+1)}{\kappa_0 T_R}\int_{T_R}^{T}\kappa(T)dT - \frac{(n+1)}{\kappa_0 T_R}\int_{T_R}^{T_W}\kappa(T)dT, \quad \text{(A1)}$$

where $\kappa(T)$ is the temperature-dependent thermal conductivity given by Eq. (6). This yields

$$\theta = (T/T_R)^{n+1} - (T_W/T_R)^{n+1}, \quad \text{(A2)}$$

where we have chosen $\theta_{\text{wall}} = 0$. The differential equation then becomes

$$\nabla^2\theta = [-(n+1)\alpha I]/\kappa_0 T_R. \quad \text{(A3)}$$

We expect only small variations of the gas temperature along the laser beam. Therefore, conductive heat transfer in the laser-beam direction (z) can be neglected and heat losses occur only radially from the beam. Using Eq. (7) with dimensionless variables $\xi = (x - x_0)/R$ and $\eta = (y - y_0)/R$, we obtain

$$\frac{\partial^2\theta}{\partial\xi^2} + \frac{\partial^2\theta}{\partial\eta^2} = -\gamma e^{-(\eta^2+\xi^2)}, \quad \text{(A4)}$$

where

$$\gamma = (n+1)\alpha W_z/\pi\kappa_0 T_R. \quad \text{(A5)}$$

For a simple geometry, Eq. (A4) can be solved analytically; however, for a complicated geometry like the one used here, numerical solutions are essential. Figure 5 shows the results of a computer calculation. The peak gas temperature θ_{peak} must depend on the substrate temperature θ_{sub} and the heat absorbed γ. Assuming a linear relation between these quantities, we get

$$\theta_{\text{peak}} = A\gamma + B\theta_{\text{sub}}, \quad \text{(A6)}$$

where A and B are geometrical factors. From the definition of θ, Eq. (A2), we find

$$\left(\frac{T_g}{aT_R}\right)^{n+1} - \left(\frac{T_s}{bT_R}\right)^{n+1} - \left(\frac{T_w}{cT_R}\right)^{n+1} = \frac{(n+1)\alpha W_z}{\pi\kappa_0 T_R} = \gamma, \quad \text{(A7)}$$

where a, b, and c are geometrical factors. The computer calculations indicate that the peak gas temperature follows Eq. (A7) exactly if we choose $a = 0.9566$, $b = 1.1152$, and $c = 1.9328$. These geometrical factors are independent of the molecular characteristics and the substrate temperature. Changing the gas mixture should only modify the value of γ. Equation (A7) is used in the text as Eq. (8).

[1]H. Fritzche, Solar Energy Mater. **3**, 447 (1980).
[2]J. C. Knights, R. A. Lujan, M. P. Rosenblum, R. A. Street, D. K. Biegelsen, and J. A. Reimer, Appl. Phys. Lett. **38**, 331 (1981).
[3]B. A. Scott, J. A. Reimer, R. M. Plecenik, E. E. Simonyi, and W. Reuter, Appl. Phys. Lett. **40**, 973 (1982).
[4]W. Paul, Solar Energy Mater. **4**, 229 (1981).
[5]M. Hirose, J. Phys. (Paris) Colloq. **C4**, 705 (1981).
[6]S. C. Gau, B. R. Weinberger, M. Akhtar, Z. Kiss, and A. G. MacDiarmid, Appl. Phys. Lett. **39**, 439 (1981).
[7]T. R. Gattuso, M. Meunier, D. Adler, and J. S. Haggerty, Materials Research Society Symposia Proceedings, *Laser Diagnostics and Photochemical Processing for Semiconductor Devices* (North-Holland, Amsterdam, 1983), Vol. 17, p. 215.
[8]M. Meunier, T. R. Gattuso, D. Adler, and J. S. Haggerty, Appl. Phys. Lett. **43**, 273 (1983).
[9]M. Meunier, J. H. Flint, D. Adler, and J. S. Haggerty, J. Non-Cryst. Solids **59–60**, 699 (1983).
[10]M. Meunier, J. H. Flint, D. Adler, and J. S. Haggerty, *Laser-Controlled Chemical Processing of Surfaces*, edited by A. W. Johnson (Elsevier, New York, 1984), p. 397.
[11]B. A. Scott, R. M. Plecenik, and E. E. Simonyi, J. Phys. (Paris) Colloq. **C4**, 635 (1981).
[12]B. A. Scott, R. M. Plecenik, and E. E. Simonyi, Appl. Phys. Lett. **39**, 73 (1981).
[13]B. S. Meyerson, B. A. Scott, and D. J. Wolford, J. Appl. Phys. **54**, 1461 (1983).
[14]D. J. Ehrlich and J. Y. Tsao, J. Vac. Sci. Technol. B **1**, 969 (1983).
[15]M. Hanabusa, A. Namiki, and K. Yoshihara, Appl. Phys. Lett. **35**, 626 (1979).
[16]M. Hanabusa, S. Moriyama, and H. Kikuchi, Thin Solid Films **107**, 227 (1983).
[17]R. Bilenchi and M. Musci, *Proceedings of the Eighth International Conference on Chemical Vapor Deposition* (The Electochemical Society, New York, 1981), p. 275.
[18]R. Bilenchi, I. Gianinoni, and M. Musci, J. Appl. Phys. **53**, 6479 (1982).
[19]R. Bilenchi, I. Gianinoni, M. Musci, and R. Murri, Materials Research Society Symposia Proceedings, *Laser Diagnostics and Photochemical Processing for Semiconductor Devices* (North-Holland, Amsterdam, 1983), Vol. 17, p. 199.
[20]R. Bilenchi, M. Musci, and R. Murri, in Photo-Optical Instrumentation Engineers *Laser Assisted Deposition Etching and Doping* (Bellingham, WA, 1984), Proc. Soc. Photo-Opt. Instrum. Eng. **459**, 61 (1985).
[21]M. Meunier, J. H. Flint, J. S. Haggerty, and D. Adler, J. Appl. Phys. 62, 2822 (1987).

Downloaded 10 May 2002 to 132.207.124.22. Redistribution subject to AIP license or copyright, see http://ojps.aip.org/japo/japcr.jsp

[22]A. C. G. Mitchell and M. W. Zemansky, *Resonance Radiation and Excited Atoms* (Cambridge University Press, Cambridge, 1961).
[23]T. F. Deutsch, J. Chem. Phys. **70**, 1187 (1979).
[24]J. W. C. Johns and W. A. Kreiner, J. Molec. Spectrosc. **60**, 400 (1976).
[25]C. D. Cody, C. R. Wronski, B. Abeles, R. B. Stephens, and B. Brooks, Solar Cells **2**, 227 (1980).
[26]R. D. Levine and R. B. Bernstein, *Molecular Reaction Dynamics* (Oxford University Press, New York, 1974).
[27]P. A. Longeway and F. W. Lampe, J. Am. Chem. Soc. **103**, 6813 (1981).
[28]M. Hanabusa and H. Kikuchi, Jpn. J. Appl. Phys. **22**, L712 (1983).
[29]Molecular characteristics and thermal conductivity data are from R. A. Svehla, NASA Technical Reports, No. TR R132 (1962).
[30]See, for example, V. S. Arpaci, *Conduction Heat Transfer* (Addison-Wesley, Reading, MA, 1966).
[31]C. G. Newman, H. E. O'Neal, M. A. Ring, F. Leska, and N. Shipley, Int. J. Chem. Kinet. **11**, 1167 (1979).
[32]J. H. Purnell and R. Walsh, Proc. R. Soc. London **293**, 543 (1966).
[33]M. E. Coltrin, R. J. Kee, and J. A. Miller, J. Electrochem. Soc., Solid State Sci. **133**, 1206 (1986).
[34]B. A. Scott, J. A. Reimer, and P. A. Longeway, J. Appl. Phys. **54**, 6853 (1983).
[35]P. John and J. H. Purnell, J. Chem. Soc. (Faraday I) **69**, 1455 (1973).
[36]M. Bowrey and J. H. Purnell, Proc. R. Soc. London Ser. A **321**, 341 (1971).
[37]A. J. Vanderwielen, M. A. Ringand, and H. E. O'Neal, J. Am. Chem. Soc. **97**, 993 (1975).
[38]M. Meunier, Ph.D. thesis, Massachusetts Institute of Technology (1984).
[39]J. P. M. Schmitt, J. Non-Cryst. Solids **59–60**, 649 (1983).
[40]P. A. Longeway, R. D. Estes, and H. A. Weakliem, J. Phys. Chem. **88**, 73 (1984).
[41]K. J. Sladek, J. Electrochem. Soc., Solid State Sci. **118**, 654 (1971).

Downloaded 10 May 2002 to 132.207.124.22. Redistribution subject to AIP license or copyright, see http://ojps.aip.org/japo/japcr.jsp